Assessment of AASHTO LRFD Specifications for Hybrid HPS 690W Steel I-Girders

Karl E. Barth, A.M.ASCE[1]; Jennifer E. Righman[2]; and Lora B. Freeman[3]

Abstract: This paper details research conducted to determine the applicability of the 2nd and 3rd editions of the *AASHTO LRFD Specifications* to hybrid I-girders fabricated from high-performance steel (HPS) 690W (100 ksi) flanges and HPS 480W (70 ksi) webs. Specifically, the scope of this paper is to evaluate the applicability of the negative moment capacity prediction equations for noncomposite I-girders subjected to moment gradient. This evaluation is carried out using three-dimensional nonlinear finite-element analysis to determine the ultimate bending capacity of a comprehensive suite of representative hybrid girders. In addition, a design study was conducted to assess the economical feasibility of incorporating HPS 690W (100 ksi) in traditional bridge applications. This was accomplished by designing a series of I-girders with varying ratios of span length to girder depth (L/D ratios) for a representative three-span continuous bridge. Results of this study indicate that both the 2nd and 3rd editions of the specifications may be used to conservatively predict the negative bending capacity of hybrid HPS 690W (100 ksi) girders, however increased accuracy results from use of the 3rd edition of the *AASHTO LRFD Specifications*. Thus, it is concluded that the restriction placed on girders fabricated from steel with a nominal yield strength greater than 480 MPa (70 ksi) can be safely removed. Additionally, results of the design study demonstrate that significant weight saving can result from the use of hybrid HPS 100W girders in negative bending regions, and that hybrid HPS 690W/HPS 480W girders may be ideally suited to sites with superstructure depth restrictions.

DOI: 10.1061/(ASCE)1084-0702(2007)12:3(380)

CE Database subject headings: High strength steel; Bridge design; Flexural strength; Plate girders; Load and resistance factor design; Predictions.

Introduction

Current AASHTO LRFD bridge specifications restrict the use of steels with nominal yield strengths greater than 480 MPa (70 ksi) by limiting the maximum moment capacity of these girders to the yield moment rather than the plastic moment as permitted for steels with lower yield strengths (AASHTO 2001, 2003). This limit was imposed due to an inadequate amount of research addressing the uncertainties related to the ductility and high yield ratio associated with this grade of steel. Consequently, the purpose of this study is to evaluate the moment capacity of noncomposite hybrid high-performance steel (HPS) 690 W/HPS 480W girders in negative bending in order to determine if these existing limitations can be removed.

The potential for removing these limitations is promising as previous researchers have indicated that the 1st and 2nd edition *LRFD Specifications* (AASHTO 1996, 2001, respectively) are applicable to girders fabricated from HPS 690W (100 ksi) steel (Sause and Fahnestock 2001). Unfortunately, these studies included the experimental testing of only two girder types: a compact girder and a girder with a compact flange and noncompact web. Thus there is a need for studies spanning a wider range of parameter configurations in order to thoroughly assess the applicability of the specifications to I-girders fabricated with HPS 690W (100 ksi).

This research is carried out by conducting finite-element analysis (FEA) of a matrix of hypothetical girders having HPS 690W (100 ksi) flanges and HPS 480W (70 ksi) webs. The girders are two-span continuous with 45.72 m (150 ft) spans and the parameters varied include flange and web compactness, lateral brace spacing, and percentage of web depth in compression, such that the girders span the range of feasible I-girder sections. Models of the negative bending region of each girder were analyzed using the FEA software ABAQUS. The girders are designed targeting key limits in the 3rd edition of the *AASHTO Specifications* (AASHTO 2003) and the results from the FEA of these girders were then compared against capacities calculated from the prediction equations in both the *AASHTO LRFD* 2nd and 3rd editions (AASHTO 2001, 2003, respectively). Additionally, results from design studies aimed at investigating the practicality of HPS 690W (100 ksi) steel in bridge girder applications are also provided.

Background

Current AASHTO Specifications (AASHTO 2001, 2003) limit the maximum moment capacity of sections with a nominal yield strength exceeding 480 MPa (70 ksi) to the yield moment since

[1]Associate Professor, Civil and Environmental Engineering Dept., West Virginia Univ., Morgantown, WV 26506 (corresponding author). E-mail: kebarth@mail.wvu.edu

[2]Assistant Professor, Dept. of Civil and Environmental Engineering, Univ. of Delaware, Newark, DE 19716.

[3]Structural Engineer, Parsons Brinckerhoff, Fairmont, WV 26554.

Note. Discussion open until October 1, 2007. Separate discussions must be submitted for individual papers. To extend the closing date by one month, a written request must be filed with the ASCE Managing Editor. The manuscript for this paper was submitted for review and possible publication on February 28, 2005; approved on March 31, 2006. This paper is part of the ***Journal of Bridge Engineering***, Vol. 12, No. 3, May 1, 2007. ©ASCE, ISSN 1084-0702/2007/3-380–388/$25.00.

insufficient studies have been conducted that justify permitting higher capacities for these sections. Among the concerns associated with higher strength steel are high yield ratio and reduced ductility. Specifically, the yield ratio, defined as the ratio of the yield strength to the ultimate strength, is 0.90 for HPS 690W (100 ksi) compared to approximately 0.77 for Grade 345 MPa (50 ksi) steel. The ductility of a material may be represented by the yield ratio (YR), the ratio of the strain at strain hardening to the yield strain (ϵ_{st}/ϵ_y), and the strain-hardening modulus (E_{st}). The reduced ductility of high strength steels has been studied by McDermott (1969).

McDermott (1969) performed experimental testing of nine I-beams fabricated from ASTM A514 steel, which has a nominal yield strength of 690 MPa (100 ksi). The actual yield strength of the beams ranged from 790 (115 ksi) to 880 MPa (128 ksi). Seven of these were subjected to uniform bending and the remaining two were loaded with moment gradient. The results of these tests show that, although fracture of the tension flange occurred in the two beams subjected to moment gradient, all nine of the girders exhibited sufficient ductility for use in plastically designed structures.

Sause and Fahnestock (2001) report experimental testing for two HPS 690W (100 ksi) girders conducted to investigate the behavior of these sections in negative bending. The girders were homogeneous girders designed using the AASHTO LRFD Specifications, neglecting the restriction on high strength steels. Based on this premise, one of the test girders was compact while the other had a compact flange and noncompact web; the predicted capacities of both of these girders were equal to M_p using the AASHTO Specifications in effect at the time this testing was conducted (AASHTO 2001). These specifications contained an alternative equation for computing the flexural resistance of girders with noncompact webs, often referred to as the "Q formula," which permitted girder capacities up to M_p for girders with noncompact webs. However, using current AASHTO Specifications (AASHTO 2005) the girder capacities of the compact girder are approximately equal to M_p and the capacity of the noncompact girder is approximately equal to M_y. The experimental results demonstrated the compact girder was able to achieve the plastic moment and the moment capacity of the second girder was 3% less than the plastic moment. Thus the study concluded that the AASHTO LRFD Specifications for flexural strength of negative bending regions were applicable to I-girders fabricated from HPS 690W (100 ksi). Additional testing coupled with FEA parametric studies have been conducted by Salem and Sause (2004), which also indicate that the flexural capacity of I-girders fabricated from HPS 690W (100 ksi) may be predicted reasonably well by the AASHTO LRFD Specifications.

Scope of Work

As discussed previously, the purpose of the study presented herein is to investigate the applicability of the current AASHTO Specifications for noncomposite hybrid HPS 100W I-girders in negative bending. This investigation is carried out through finite-element analysis, using a matrix of hypothetical I-girders typical of those routinely employed in bridge designs. The varied parameters are web slenderness, flange slenderness, lateral brace spacing, and percentage of web depth in compression. Furthermore, the 3rd edition of the *AASHTO Specifications* (AASHTO 2003) contains two sets of strength prediction equations for negative bending moment capacity. One of these is given is Section 6.10.8 of the specifications and the maximum moment capacity resulting from the use of these equations is equal to M_y. The second set of strength prediction equations is provided in Section 6.10 Appendix A and the maximum moment capacity resulting from the use of these equations is equal to M_p. Girders are designed in this work to target key slenderness values contained in these two sets of moment capacity equations as described below. Specifically, there are four values of web slenderness, three values of flange slenderness, four values of lateral brace spacing, and two values of percentage of web depth in compression incorporated in this work.

The parametric values used for each of the girder designs are given in Tables 1 and 2. The girder designs may be classified into two series: the Series A girders were specifically designed to evaluate Section 6.10.8 of the specifications, while the Series B girders were designed based on Appendix A. The number after the dash in the girder label refers to the target ratio of D_{cp}/D of the girder. The web, flange, and lateral bracing designations used in the table are explained in the subsequent sections.

Table 1. AASHTO LRFD Section 6.10.8 Girders

Girder label	Web	Flange	L_b Uniform	L_b Gradient	$\frac{M_{n_{2nd}}}{M_{FEA}}$	$\frac{M_{n_{3rd}}}{M_{FEA}}$
A1-0.65	Stocky	Comp.	L_p	$0.57L_{Cb}$	0.84	0.99
A2-0.65	Int.	Comp.	L_p	$0.56L_{Cb}$	0.96	0.97
A3-0.65	λ max	Comp.	L_p	$0.55L_{Cb}$	0.94	0.95
A4-0.65	Stocky	Non.	L_p	$0.59L_{Cb}$	0.49	0.79
A5-0.65	Int.	Non.	L_p	$0.57L_{Cb}$	0.47	0.88
A6-0.65	λ max	Non.	L_p	$0.56L_{Cb}$	0.37	0.82
A7-0.65	Stocky	Comp.	L_r	$0.99L_{Cb}$	0.98	1.01
A8-0.65	Int.	Comp.	L_r	$0.95L_{Cb}$	0.91	1.03
A9-0.65	λ max	Comp.	L_r	$0.93L_{Cb}$	0.92	1.01
A10-0.65	Stocky	Non.	L_r	$1.06L_{Cb}$	0.60	0.96
A11-0.65	Int.	Non.	L_r	$0.99L_{Cb}$	0.47	0.88
A12-0.65	λ max	Non.	L_r	$0.95L_{Cb}$	0.39	0.87
A13-0.65	Stocky	Comp.	L_s	$1.18L_{Cb}$	0.78	0.81
A14-0.65	Int.	Comp.	L_s	$1.10L_{Cb}$	0.74	0.85
A15-0.65	λ max	Comp.	L_s	$1.05L_{Cb}$	0.85	0.85
A16-0.65	Stocky	Non.	L_s	$1.31L_{Cb}$	0.74	0.79
A17-0.65	Int.	Non.	L_s	$1.18L_{Cb}$	0.69	0.82
A18-0.65	λ max	Non.	L_s	$1.10L_{Cb}$	0.52	0.83
A1-0.50	Stocky	Comp.	L_p	$0.56L_{Cb}$	0.90	0.98
A2-0.50	Int.	Comp.	L_p	$0.55L_{Cb}$	0.97	0.96
A3-0.50	λ max	Comp.	L_p	$0.54L_{Cb}$	0.95	0.95
A4-0.50	Stocky	Non.	L_p	$0.58L_{Cb}$	0.49	0.79
A5-0.50	Int.	Non.	L_p	$0.57L_{Cb}$	0.67	0.83
A6-0.50	λ max	Non.	L_p	$0.55L_{Cb}$	0.39	0.81
A7-0.50	Stocky	Comp.	L_r	$0.96L_{Cb}$	0.97	1.01
A8-0.50	Int.	Comp.	L_r	$0.94L_{Cb}$	0.99	0.99
A9-0.50	λ max	Comp.	L_r	$0.93L_{Cb}$	0.95	1.02
A10-0.50	Stocky	Non.	L_r	$1.01L_{Cb}$	0.37	0.87
A11-0.50	Int.	Non.	L_r	$0.97L_{Cb}$	0.47	0.84
A12-0.50	λ max	Non.	L_r	$0.95L_{Cb}$	0.39	0.81
A13-0.50	Stocky	Comp.	L_s	$1.12L_{Cb}$	0.81	0.81
A14-0.50	Int.	Comp.	L_s	$1.08L_{Cb}$	0.87	0.86
A15-0.50	λ max	Comp.	L_s	$1.05L_{Cb}$	0.78	0.80
A16-0.50	Stocky	Non.	L_s	$1.21L_{Cb}$	0.77	0.79
A17-0.50	Int.	Non.	L_s	$1.14L_{Cb}$	0.73	0.84
A18-0.50	λ max	Non.	L_s	$1.09L_{Cb}$	0.52	0.79

Table 2. AASHTO LRFD Appendix A Girders

Girder	Web	Flange	L_b Uniform	L_b Gradient	$\frac{M_{n_{2nd}}}{M_{FEA}}$	$\frac{M_{n_{3rd}}}{M_{FEA}}$
B1-0.65	Comp.	Comp.	L_p	$0.66L_{Cb}$	0.80	0.98
B2-0.65	Non.	Comp.	L_p	$0.55L_{Cb}$	0.96	0.97
B3-0.65	Comp.	Non.	L_p	$0.71L_{Cb}$	0.47	0.76
B4-0.65	Non.	Non.	L_p	$0.57L_{Cb}$	0.42	0.85
B5-0.65	Comp.	Comp.	L_r	$1.34L_{Cb}$	0.95	0.98
B6-0.65	Non.	Comp.	L_r	$0.93L_{Cb}$	0.90	1.04
B7-0.65	Comp.	Non.	L_r	$1.54L_{Cb}$	0.63	1.01
B8-0.65	Non.	Non.	L_r	$0.99L_{Cb}$	0.42	0.85
B9-0.65	Comp.	Comp.	L_s	$1.63L_{Cb}$	0.77	0.80
B10-0.65	Non.	Comp.	L_s	$1.07L_{Cb}$	0.74	0.85
B11-0.65	Comp.	Non.	L_s	$2.03L_{Cb}$	0.73	0.79
B12-0.65	Non.	Non.	L_s	$1.17L_{Cb}$	0.69	0.82
B1-0.50	Comp.	Comp.	L_p	$0.60L_{Cb}$	0.91	0.99
B2-0.50	Non.	Comp.	L_p	$0.54L_{Cb}$	0.97	0.96
B3-0.50	Comp.	Non.	L_p	$0.63L_{Cb}$	0.44	0.77
B4-0.50	Non.	Non.	L_p	$0.56L_{Cb}$	0.42	0.82
B5-0.50	Comp.	Comp.	L_r	$1.08L_{Cb}$	0.93	0.96
B6-0.50	Non.	Comp.	L_r	$0.93L_{Cb}$	1.03	1.02
B7-0.50	Comp.	Non.	L_r	$1.18L_{Cb}$	0.48	0.85
B8-0.50	Non.	Non.	L_r	$0.97L_{Cb}$	0.43	0.83
B9-0.50	Comp.	Comp.	L_s	$1.26L_{Cb}$	0.89	0.89
B10-0.50	Non.	Comp.	L_s	$1.06L_{Cb}$	0.87	0.86
B11-0.50	Comp.	Non.	L_s	$1.44L_{Cb}$	0.77	0.80
B12-0.50	Non.	Non.	L_s	$1.14L_{Cb}$	0.67	0.83

All girders have a constant span-to-depth ratio of 30, cross-section aspect ratio, D/b_{fc}, of 4, and are comprised of hybrid configurations with HPS 480W (70 ksi) webs and HPS 690W (100 ksi) flanges. Transverse stiffeners were used where necessary to provide sufficient shear capacity.

Web Slenderness Limits

Four alternative web slenderness limits are targeted in this work as discussed below. Two of these limits are found in Appendix A of Section 6.10. These are the compact limits intended to provide minimum moment capacities of M_p and the noncompact limit, which is the maximum allowable web slenderness permissible in order for Appendix A to be valid. A series of girders were also designed at the maximum allowable web slenderness permitted by Section 6.10.2 of the AASHTO 3rd edition specifications. Finally, an intermediate web slenderness value was incorporated to evaluate the influence of this parameter on the strength prediction equations given in Section 6.10.8. As a result, the compact web limit from the 2nd edition of the specifications (AASHTO 2001) is included in the parametric study for the evaluation of moment capacities computed using Section 6.10.8.

1. Compact: Sections that meet the compact web requirement, which are labeled Comp. in Tables 1 and 2, are expected to develop M_p provided flange slenderness and lateral brace spacing requirements are satisfied. Article A6.2.1 defines the maximum web slenderness for compact webs by Eq. (1), where D_{cp}=depth of web in compression, t_w=web thickness, E is the elastic modulus, F_{yc}=yield strength of the compression flange, and R_h=hybrid factor

$$\frac{2D_{cp}}{t_w} = \frac{\sqrt{\frac{E}{F_{yc}}}}{\left(0.54\frac{M_p}{R_h M_y} - 0.09\right)^2} \tag{1}$$

It is noted that slightly higher web slenderness values than given by Eq. (1) were used for the compact girders in this study. This is because the girders in this study were designed based on draft specifications, which specified the second term in the numerator to be equal to 0.10 instead of 0.09.

2. Stocky: Several girders in this study were designed to have stocky webs. This designation refers to webs designed at the compact limit as defined by the 2nd edition of the LRFD bridge specifications. Webs with this designation satisfy Eq. (2) given below

$$\frac{2D_{cp}}{t_w} \leq 3.76\sqrt{\frac{E}{F_{yc}}} \tag{2}$$

3. Noncompact: Sections in which the web slenderness satisfies Eq. (3) are classified as having an intermediate web slenderness (labeled Non. in Table 2), where D_c=depth of web in compression in the elastic range. This limit is taken from the requirements in Section A6.1 (AASHTO 2003)

$$\frac{2D_c}{t_w} \leq 5.7\sqrt{\frac{E}{F_{yc}}} \tag{3}$$

4. Slender: The maximum web slenderness (λ_{max}) permitted by the specifications for I-girders without longitudinal stiffeners is given in Eq. (4), where D is the web depth. This limit is given in Article 6.10.2.1.1 of the specifications and is intended to limit the web proportions to practical limits

$$\frac{D}{t_w} \leq 150 \tag{4}$$

Flange Slenderness Limits

Three flange limits, discussed below, are used in this work. Both Section 6.10.8 and Appendix A utilize the same compact web limit, which is also implemented in this work. Conversely, Section 6.10.8 and Appendix A provide alternative definitions of noncompact flanges, which are labeled "noncompact–6.10.8" and "noncompact–Appendix A" below. Additionally, both noncompact flange limits are also limited to the maximum permissible flange slenderness as discussed below.

1. Compact: Sections designed to meet the compact flange slenderness limit are expected to reach M_p provided other requirements on web slenderness and lateral bracing distance are also satisfied. The compact flange slenderness limit is defined in Articles 6.10.8.2.2 and A6.3.2, and is given below, where b_{fc} and t_{fc} are the width and thickness of the compression flange, respectively

$$\frac{b_{fc}}{2t_{fc}} \leq 0.38\sqrt{\frac{E}{F_{yc}}} \tag{5}$$

2. Noncompact–6.10.8: The noncompact flange limit given below, Eq. (6), represents the point at which elastic buckling of the compression flange begins to occur. In this equation F_{yr}=smaller of the compression flange yield stress with the

consideration of residual stress effects or the nominal yield strength of the web. This limit is discussed in Article 6.10.8.2.2 of the AASHTO Specifications

$$\frac{b_{fc}}{2t_{fc}} \leq 0.56\sqrt{\frac{E}{F_{yr}}} \tag{6}$$

3. Noncompact–Appendix A: Article A6.3.2 outlines the noncompact flange slenderness limit, given in Eq. (7), which is the maximum flange slenderness at which a linear relationship exists between flange slenderness and moment capacity, where k_c=flange local buckling coefficient

$$\frac{b_{fc}}{2t_{fc}} \leq 0.95\sqrt{\frac{Ek_c}{F_{yr}}} \tag{7}$$

All flanges must also satisfy Eq. (8), which is intended to prevent excessive distortions of the flange when welded to the web. Therefore, the noncompact flanges designed in this work have a flange slenderness equal to the minimum of either Eqs. (6) and (8) or Eqs. (7) and (8)

$$\frac{b_{fc}}{2t_{fc}} \leq 12.0 \tag{8}$$

Lateral Bracing Limits

Four different lateral bracing distances were incorporated in this work. As with the flange slenderness limits discussed above, Appendix A and Section 6.10.8 implement the same definition of compact lateral brace spacing. This brace spacing is also used and referred to as compact in this work. Furthermore, alternative classifications of noncompact brace spacing are used in Section 6.10.8 and Appendix A. Both of these limits are used in this work and are referred to as noncompact—Section 6.10.8 and noncompact—Appendix A. A fourth lateral bracing limit is also considered, which is equal to an upper bound of the maximum lateral bracing distance likely in typical bridge construction.

1. Compact: The lateral brace spacing that is defined using Eq. (9) is the compact brace spacing (L_p), which corresponds to the brace spacing at which lateral–torsional buckling occurs under uniform moment. This spacing is discussed in Articles 6.10.8.2.3 and A6.3.3, where the symbol r_t is the effective radius of gyration for lateral torsional buckling

$$L_p = r_t\sqrt{\frac{E}{F_{yc}}} \tag{9}$$

2. Noncompact - 6.10.8: The noncompact lateral brace spacing (L_r) given in Section 6.10.8.2.3 is calculated from Eq. (10), and corresponds to the point at which sections in uniform bending are expected to fail by elastically buckling (neglecting St. Venant effects)

$$L_r = \pi r_t\sqrt{\frac{E}{F_{yr}}} \tag{10}$$

3. Noncompact–Appendix A: Eq. (11) gives the noncompact brace spacing as determined from Article A6.3.3 of Appendix A, where J is the St. Venant torsional constant, S_{xc} is the elastic section modulus, and h is the depth between the centerline of the flanges. Thus, this equation represents the brace spacing at which beams subjected to uniform moment will elastically buckle considering the St. Venant effect

$$L_r = 1.95r_t\frac{E}{F_{yr}}\sqrt{\frac{J}{S_{xc}h}}\sqrt{1+\sqrt{1+6.76\left(\frac{F_{yr}}{E}\frac{S_{xc}h}{J}\right)^2}} \tag{11}$$

4. Slender: AASHTO Specifications do not set a limit on maximum allowable lateral brace spacing; however, a lateral bracing distance of 9.114 m (30 ft) was believed to be a reasonable upper-bound bracing distance of that used in typical bridge construction as girders designed with larger bracing distances may require impractical cross sections in order to satisfy constructibility requirements. Therefore, several girders in this study were designed with a lateral bracing distance of 9.144 m (30 ft), which is labeled as slender bracing distance (L_s).
5. Moment gradient effect: The girders included in the parametric study discussed herein were proportioned to have unbraced lengths equal to the limits given above. However, it should be realized that Eqs. (9)–(11) are based on uniform bending conditions, while the girders in this study are subjected to moment gradient conditions. The maximum allowable lateral bracing distance that will result in the maximum capacity allowed by Section 6.10.8 is equal to the following

$$L_{C_b} = L_p + \frac{\left(1-\frac{1}{C_b}\right)(L_r - L_p)}{\left(1-\frac{F_{yr}}{R_h F_{yc}}\right)} \tag{12}$$

Similarly, the maximum allowable lateral bracing distance that will result in the maximum capacity allowed by Appendix A is given by Eq. (13)

$$L_{C_b} = L_p + \frac{\left(1-\frac{1}{C_b}\right)(L_r - L_p)}{\left(1-\frac{F_{yr}S_{xc}}{R_{pc}M_{yc}}\right)} \tag{13}$$

The lateral bracing distances of each girder are expressed as a function of Eqs. (12) and (13), as applicable, in Tables 1 and 2 under the heading "L_b gradient," while the heading "L_b uniform" designates the lateral bracing rule used in the FEA. For example, Girder A1-0.65 has a lateral bracing distance equal to L_p, which is also equal to 57% of L_{Cb}. This means that the maximum moment capacities of the girder may be achieved at bracing distance that is 1/0.57 or 75% greater than the compact bracing distance. Reviewing this data for all parametric girders shows similar trends. It is also observed that, for the girders included in this work, the maximum moment capacities can be obtained at lateral bracing distances that are approximately equal to L_r.

Depth of Web in Compression Limits

The effects of the ratio of D_{cp}/D were investigated since previous studies have determined the ratio has a significant influence on the behavior of I-girder sections (Barth and White 1998). Two D_{cp}/D ratios were used in this study: 0.50, representing a doubly symmetric girder and 0.65, representing an upper bound of typical D_{cp}/D ratios encountered in practical bridge designs.

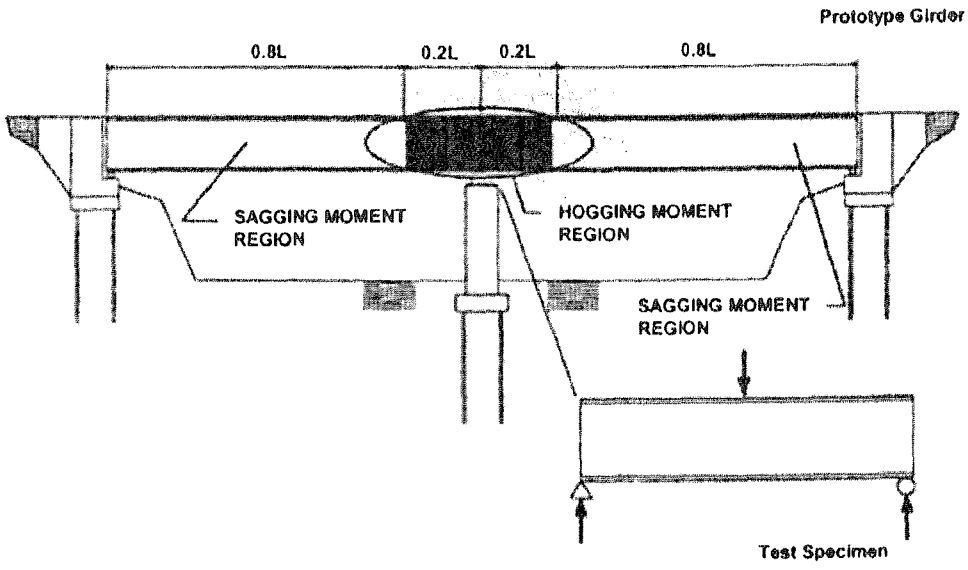

Fig. 1. Typical two-span highway bridge

Finite-Element Analysis

As previously discussed, this study focuses on the flexural capacity of negative bending regions. Therefore, models were developed to represent the hogging moment region of continuous girders, as shown in Fig. 1. These models are simply supported in three-point bending, where the concentrated load represents the pier reaction and the simple supports correspond to the points of contraflexure of the continuous girder. For this study, the distance from the pier to the inflection points is assumed to be $0.2L$, where L is the span length; therefore, since the span length of the girders is assumed to be 45.72 m (150 ft), the girder models are 18.288 m (60 ft) in length. This same approach has been used by Barth et al. (2000) in an earlier study evaluating the rotation capacity of HPS 480W (70 ksi) I-girders.

The girders were modeled using general purpose shell elements with reduced integration (ABAQUS S4R). A relatively high mesh density is used consisting of ten elements across the flange width, and 20 elements through the depth of the web. The aspect ratio of the compression flange elements near the center of the span was approximately one, and an increasing element length was used in regions of the girder away from the point of the applied load such that the largest compression flange aspect ratio was two, which occurred in the ends of the girder. Appropriate constraints were applied to model the simply supported boundary conditions as well as lateral bracing. These consist of vertical constraints at the bearing locations at each end of the beam, longitudinal constraints at one bearing, and lateral constraints of the web nodes where lateral braces are assumed. A minimum of four lateral bracing segments are used in each girder to provide torsional restraint to the girder cross section.

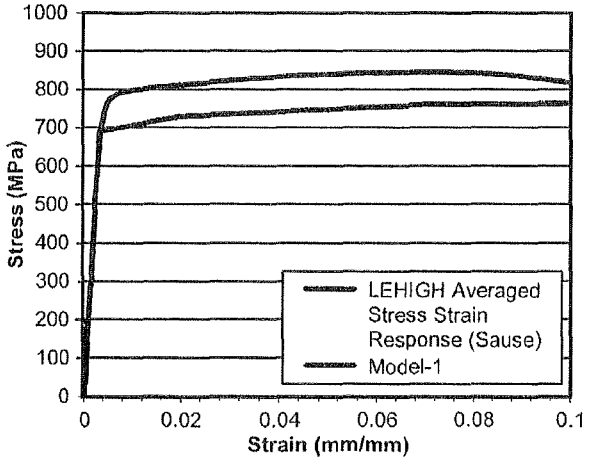

Fig. 2. 690 MPa engineering stress–strain material model

Nonlinear material properties based on experimental testing were incorporated in the FEA. Specifically, experimental data from Lehigh University (Salem and Sause 2004) was used to develop the 690 MPa (100 ksi) constitutive model used in this work. As shown in Fig. 2, the original engineering stress versus engineering strain data is scaled such that the yield strength coincided with 690 MPa (100 ksi) since a higher yield strength was obtained in the experimental testing. An elastic modulus of 200,000 MPa (29,000 ksi), a YR of 0.91, and a strain hardening modulus of 646 MPa (93.7 ksi), are also used in the material model. The constitutive properties for HPS 480W (70 ksi) used in this work are based on experimental testing conducted by the Federal Highway Administration (Wright, personal communication 1997) (see Fig. 3). Again, the actual test data have been scaled such that the yield strength of the material corresponds to 480 MPa (70 ksi). The constitutive model has a YR of 0.83, a modulus of elasticity of 200,000 MPa (29,000 ksi), and a strain-hardening modulus of 4,964 MPa (720 ksi). These experimental data, which are reported in terms of engineering stress and engineering strain, are then converted into true stress and true strain are required for input into ABAQUS (ABAQUS 2004).

Residual stresses resulting from welding and flame cutting processes have a significant influence on the section. These residual stresses are characterized by large tensile stresses at the location of the web to flange weld and smaller equilibrating forces away from the web–flange junction. Therefore, longitudinal residual stresses were incorporated into the girder models using the stress pattern depicted in Fig. 4. This stress distribution is based on the residual stresses assumed by White et al. (2001). Specifically, the compressive residual stresses used here are the

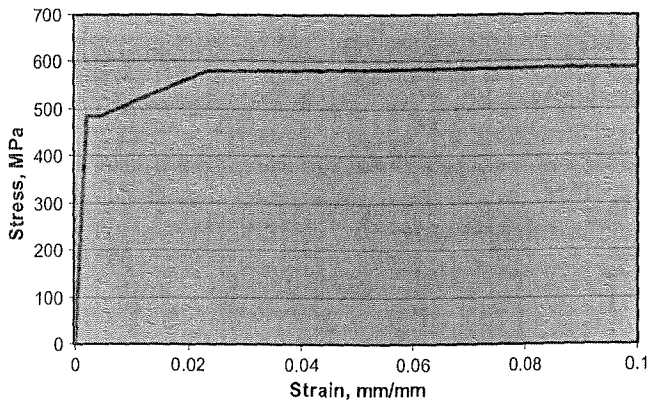

Fig. 3. 480 MPa engineering stress–strain material model

same as those used by White et al., while the tensile residual stresses are slightly altered such that equilibrium is satisfied.

The modified Riks method was employed to capture the load–deflection curve of each girder. Because the modified Riks method requires a continuous response during the analysis, initial imperfections were applied to perturb the system in order to provide numerical stability and avoid bifurcation buckling. Initial geometric imperfections, based on maximum allowable tolerances specified by the American Welding Society (AWS) and engineering judgment, are also incorporated into the FEA. Specifically, three types of geometric imperfections are included in the FEA: an initial out-of-flatness of each web panel [Fig. 5(a)], an initial tilt of the compression flange within each web panel [Fig. 5(b)], and an initial sweep of the compression flange within each unbraced length [Fig. 5(c)]. A web panel is defined as the entire web depth laterally bounded by transverse stiffener locations.

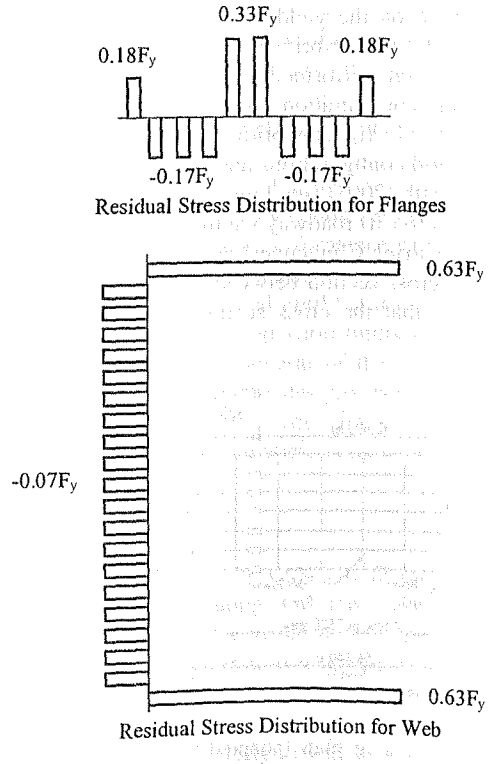

Fig. 4. Residual stress pattern

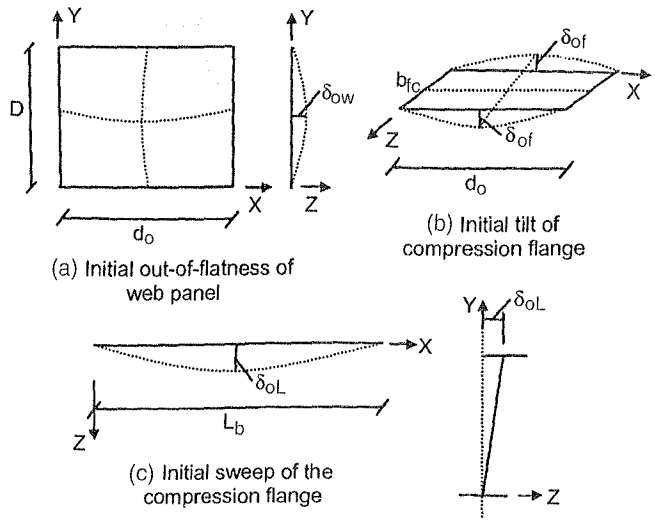

Fig. 5. Geometric imperfections

In this study, the maximum initial out-of-flatness of the web, δ_{0w}, is prescribed to be equal to $d/100$, where d is the minimum panel dimension, either the web depth or distance between stiffeners. The maximum allowable tilt of the flanges, δ_{of}, is assigned to be the lesser value of $b_{fc}/150$ or $0.3d_0/150$, where d_0 is the distance between transverse stiffeners. A lateral sweep of the compression flange (δ_{0L}) is specified with a maximum value equal to $L_b/1{,}500$, where L_b is the distance between lateral bracing. These maximum values occur at the locations indicated in Fig. 5 and vary throughout the girder in a sine-wave or linear relationship (see Fig. 5). Furthermore, the direction in which the imperfections are applied alternates in adjacent panels, where δ_{0L} and δ_{0w} are prescribed in the same direction within each web panel so that the effects of these two imperfections are cumulative.

While these imperfection values are thought to be a reasonable approximation of the actual imperfections that occur in typical welded girders, it was necessary to apply increased values of imperfections in the analyses of two of the girders considered in this study in order to avoid numerical difficulties. These girders are labeled as A-15-0.65 and A-18-0.50 in Table 1 and are two of the four girders that have both slender webs and slender lateral brace spacing. The flange and lateral imperfections in girder A-18-0.50 were increased by approximately 60% compared to the values presented above in the two panels adjacent to the midspan of the girder. A more dramatic increase in imperfections was required in all panels of girder A-15-0.65 where the lateral imperfections were increased by an average of 66%, the flange imperfections were increased an average of 78%, and the web imperfections were increased an average of 32%. These increased imperfection values result in more conservative maximum moment capacity predictions.

Results of Study

All of the girders met or exceeded the capacities calculated using both the 2nd and 3rd editions of the AASHTO LRFD within acceptable limits. The moment capacities resulting from the FEA of each girder are presented in Table 1 where M_{n2nd}/M_{FEA} refers to the ratio of the moment capacity predicted by the 2nd edition to the moment capacity predicted by the FEA analysis and

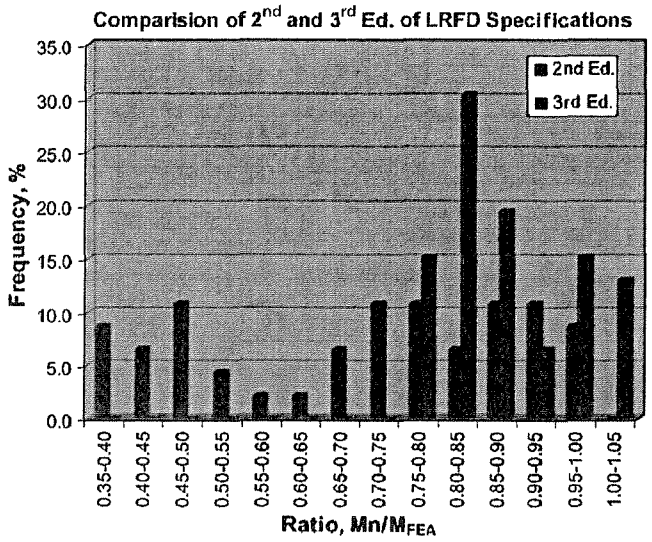

Fig. 6. Comparison of 2nd and 3rd editions of LRFD specifications

M_{n3rd}/M_{FEA} refers to the moment capacity predicted by the 3rd edition divided by the moment capacity predicted by the FEA. For the computation of M_{n3rd}/M_{FEA}, the flexural capacity equations provided in Appendix A are used in all cases except for girders having "maximum" web slenderness. The capacities of girders with maximum web slenderness are computed using Section 6.10.8 as the Appendix is not valid for girders with web slenderness values exceeding Eq. (3).

Using the 3rd edition, the average ratio of the predicted capacity to the FEA results (M_{n3rd}/M_{FEA}) is 0.88, while the low is 0.76 and the maximum is 1.03. Thus, a few sections were unable to meet the estimated flexural capacity, but were within 3%, which the writers considered to be an acceptable level of accuracy. All of these sections that were unable to achieve the moment capacity predicted by AASHTO had noncompact lateral bracing, and the majority had a compact compression flange. Using the 3rd edition, the lowest strength ratios result for girders with a slender bracing distance; the average for these girders is 0.82.

The average M_{n2nd}/M_{FEA} for the 2nd edition of the specifications is 0.71, which is 17% less than the average computed using the 3rd edition. The values of M_{n2nd}/M_{FEA} range between a maximum of 0.99 and a minimum of 0.37. As indicated by this low minimum value, the 2nd edition of the AASHTO LRFD significantly underestimates the flexural capacity of several girders. In general these girders have a noncompact compression flange and compact or noncompact lateral bracing distance; the average M_n/M_{FEA} for this class of girders is 0.46. Furthermore, there are three prediction equations that equally contribute to these low strength ratios. These are equations 6.10.4.2.4a-2 (which governs for girders with a compact lateral bracing distance); 6.10.4.2.6a-1 (the controlling lateral torsional buckling equation for girders with webs satisfying $2D_c/t_w \leq 5.76\sqrt{E/F_{yc}}$ for doubly symmetric girders or $2D_c/t_w \leq 4.64\sqrt{E/F_{yc}}$ for monosymmetric girders); and 6.10.4.2.6a-2 (the controlling lateral torsional buckling equation for noncompact bracing distance when the above web limits are not satisfied).

The FEA results are compared with the capacities predicted from the 2nd and 3rd editions in graphical form in Fig. 6. Here it is shown that the 3rd edition yields a considerably more accurate estimate of the flexural capacity of the hybrid girders than the 2nd edition. Furthermore, the capacity of girders with a noncompact flange has been shown to be drastically underestimated by the 2nd edition; by comparison the ratio of M_{n3rd}/M_{FEA} is 0.84 for this same class of girders.

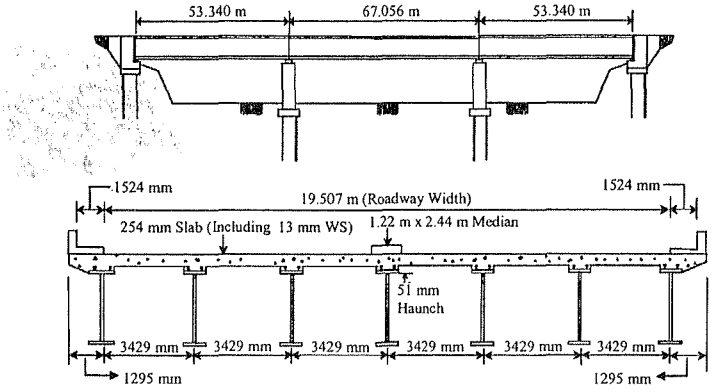

Fig. 7. Bridge profile and cross section (adapted from Clingenpeel 2001)

In conclusion, the estimated capacities from the 3rd edition of the specifications were deemed to be accurate yet conservative predictions of the girder's ultimate capacity, while the 2nd edition of the specifications gives less accurate predictions, particularly for girders with noncompact flanges. Thus, it is concluded that removing the limitations placed on hybrid HPS 100W girders in the 3rd edition specifications is justified and would result in an adequate margin of safety.

Design Study

Scope of Design Study

The purpose of the design study is to determine the practicality of HPS 100W hybrid girder configurations for bridge design if the restriction based on the yield stress was removed from the 3rd edition of the AASHTO bridge specifications (AASHTO 2003). Girder designs were performed for a three-span continuous bridge with a span configuration of 53.34 m–67.056 m–53.34 m (175 ft–220 ft–175 ft). This bridge was previously optimized for HPS 70W hybrid configurations and is discussed in detail in Clingenpeel and Barth (2003) (see Figs. 7 and 8). The five-lane bridge with a 19.50 m (64 ft) roadway width has sidewalks on both sides and a median barrier. Clingenpeel and Barth varied the number of girders in the cross section between seven and nine in the study, and concluded that the cross section with the least number of

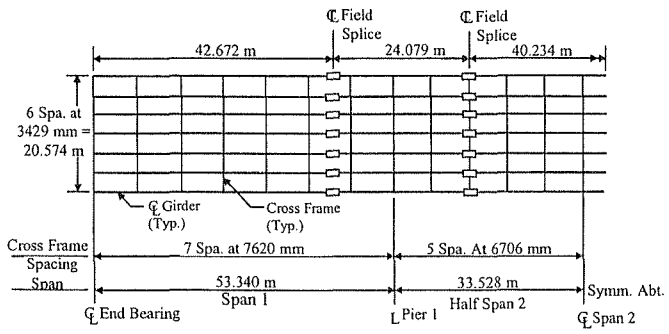

Fig. 8. Girder framing plan (adapted from Clingenpeel and Barth 2003)

girder lines yielded the most economical design. Therefore, the bridge system designed in this study has seven girders spaced at 3,429 mm (11 ft 3 in.). The hybrid girders have HPS 690W (100 ksi) flanges in the negative bending region and HPS 480W (70 ksi) in all other locations. Transitions in flange width were only permitted at the location of a bolted field splice, while flange transitions in thickness were included 4,572 mm (15 ft) away from the pier if a weight savings of more than 408 kg (900 lb) was achieved.

The following is a list of additional parameters that were held constant during the study:

- HL-93 live loading;
- Interior girder design;
- Stay-in-place metal forms=718 N/m^2 (15 psf);
- Future wearing surface=1,197 N/m^2 (25 psf);
- Parapet plus railing weight=4.82 kN/m (330 lb/ft);
- Median=4.38 kN/m (300 lb\ft);
- Sidewalk loading=9.34 kN/m (640 lb\ft);
- Cross frame spacing: seven spaces at 7,620 mm (25 ft) in Spans 1 and 3, and ten spaces at 6,706 mm (22 ft) in Span 2; and
- 5% increase in girder dead load for miscellaneous steel.

The concrete deck slab was taken to be 254 mm (10 in.) thick, and the haunch, which includes the top flange thickness, was assumed to be 50.8 mm (2 in.).

Design Process

Designs were developed for six span-to-depth (L/D) ratios ranging from 15 to 40 in increments of 5. For the purpose of this study, the span length, L, was taken as the longest span length, 67.056 m (220 ft), and the depth, D, is the entire superstructure depth. For a given L/D ratio, the initial flange width was selected such that D_w/b_f fell in the range of 3.0 and 6.0, where D_w is the depth of the web and b_f is the flange width. The upper limit of 6.0 is stated in the 3rd edition of the specifications in Article 6.10.2.2 (AASHTO 2003). The web thickness was selected based on the geometric proportion limits or a partially stiffened web approach, in which the thickness that requires no stiffeners was determined and then reduced by 1.59 mm (1/16 in.) to 3.175 mm (1/8 in). In addition, the web thickness and depth remained constant for a given girder.

For a given L/D ratio, an initial design was analyzed to determine the performance ratios by neglecting the yield stress restriction on high strength steel. If a performance ratio less than 1.0 was obtained, the bridge was redesigned using a smaller cross section. This process was repeated until the minimum weight design satisfying the geometric proportion limits in Section 6.10.2 was obtained. It is noted that several of the designs were controlled by these limits; because the designs were based on a fixed web depth, the cross-section proportion limits then dictate minimum sizes for several other geometric parameters.

Results

Fig. 9 shows the girder weight versus L/D ratio for the HPS 100W girders in this study along with the results from Clingenpeel and Barth (2003). Similar to the present study, Clingenpeel and Barth investigated the variation in girder weight versus L/D ratio, although for homogeneous HPS 480W (70 ksi) girders. Fig. 9 shows significant weight savings result from the use of the hybrid HPS 690W (100 ksi) design over the HPS 480W (70 ksi) design, especially for shallower superstructure depths. At L/D ratio of 35 there is a 31.0% difference in weight between the hybrid HPS 690W (100 ksi) design and the homogeneous HPS 480W (70 ksi) girder. Also note the lightest HPS 480W (70 ksi) girder system weighs 23.9% more than the lightest hybrid HPS 690W (100 ksi) design. Clingenpeel and Barth (2003) also present the results of a hybrid Grade 345/HPS 480W with a L/D ratio of 27.5, which is determined to be the optimum L/D ratio for this configuration. The girder weight resulting from this design is 18.7% higher than the weight of the optimum HPS 480/690W hybrid girder, as shown in Fig. 9.

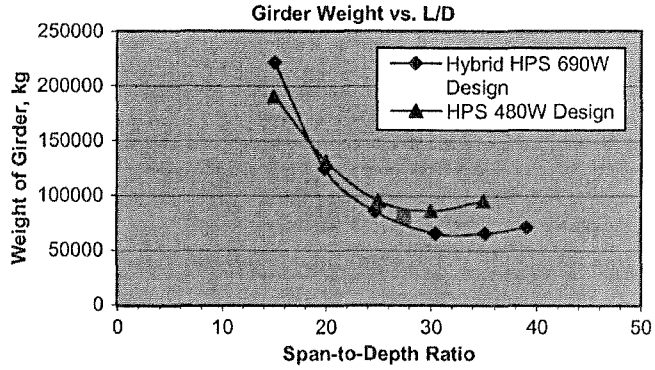

Fig. 9. Comparison of hybrid HPS 690W (100 ksi) designs with HPS 480W (70 ksi) designs

All of the hybrid HPS 690W (100 ksi) girder designs weigh less than the HPS 480W (70 ksi) designs except for one. Specifically, the HPS 690W (100 ksi) design for $L/D=15$ weighs more than the HPS 480W (70 ksi) design due to changes in the specifications. The study conducted by Clingenpeel and Barth (2003) was governed by the 2nd edition of the *AASHTO LRFD Specifications*, and the designs in the present study were based on the 3rd edition. The hybrid HPS 690W (100 ksi) girder design with a $L/D=15$ was controlled by the geometric proportion limits incorporated into the 3rd edition of the specifications in Section 6.10.2. These limits have the most significant effect on girders with low L/D ratios and have a decreasing influence as the L/D ratio increases. The design with the smallest L/D ratio that is not influenced by the geometric proportions limit is $L/D=30$.

It is also apparent from Fig. 9 that the optimum L/D ratio is larger for the hybrid HPS 690W (100 ksi) designs than for the HPS 480W (70 ksi) designs. Specifically, the optimal L/D ratio for the HPS 480W (70 ksi) study was 27.5, while this value is approximately 32.2 for the hybrid HPS 690W (100 ksi) configuration. This trend is typical for high strength steels since the increased strength allows for lighter sections at shallower superstructure depths. It should be noted that although this results in economical savings from a strength perspective, one potential negative consequence of these higher optimum L/D ratios and shallower superstructure depths for HPS 690W (100 ksi) is the smaller moment of inertia values for the girders, which result in increased deflections and vibrations.

Summary and Conclusions

Extensive FEA modeling has been conducted to evaluate the restrictions placed on girders fabricated from HPS 690W (100 ksi) in the current AASHTO Specifications. This evaluation has shown that the negative flexural capacity of noncomposite hybrid HPS 690W (100 ksi) girders subjected to moment gradient is ac-

curately predicted by the 3rd edition *AASHTO LRFD Specifications*. Thus it is recommended that the limitation imposed on the maximum allowable nominal yield stress of these types of sections can be safely removed from the specifications.

The 2nd edition of the specifications also safely predict the capacity of HPS 690W (100 ksi) girders. However, the flexural capacity of the high strength I-girders with noncompact flanges predicted by the 2nd edition is overly conservative.

The results of the design study illustrate that hybrid HPS 690W (100 ksi) girders may be used to obtain efficient bridge systems. Even though many of the sections were controlled by the geometric proportion limits, the girders were able to achieve a weight savings over the homogeneous HPS 480W (70 ksi) girder designs, with one exception. Furthermore, the increased strength contributed to an increase in the optimum L/D ratio for the hybrid HPS 690W (100 ksi) girders to approximately 32.2 compared to 27.5. Therefore, hybrid HPS 690W (100 ksi) configurations would be ideal for bridge sites that have a restricted superstructure depth.

References

AASHTO. (1996). *LRFD bridge design specifications*, 1st Ed., Washington, D.C.

AASHTO. (2001). *LRFD bridge design specifications*, 2nd Ed., Washington, D.C.

AASHTO. (2003). *LRFD bridge design specifications*, 3rd Ed., Washington, D.C.

ABAQUS. (2002). *ABAQUS/standard user' manual, version 6.3*, Hibbitt, Karlsson & Sorensen, Inc.

Barth, K. E., and White, D. W. (1998). "Finite element evaluation of pier moment-rotation characteristics in continuous-span steel I girders." *Eng. Struct.*, 20(8), 761–778.

Barth, K. E., White, D. W., and Bobb, B. M. (2000). "Negative bending resistance of HPS70W girders." *J. Constr. Steel Res.* 53, 1–31.

Clingenpeel, B. F. (2001). "Economical use of high performance steel in slab-on-steel stringer bridge design." MS thesis, West Virginia Univ., Morgantown, W. Va.

Clingenpeel, B. F., and Barth, K. E., (2003). "Design optimization study of a three-span continuous bridge using HPS70W." *Eng. J.*, 39(3), 121–126.

Salem, E. S., and Sause R. (2004). "Flexural strength and ductility of highway bridges fabricated from HPS-100W steel." *ATLSS Rep. No. 04-12*, Center for Advanced Technology for Large Structural Systems, Lehigh Univ., Bethlehem, Pa.

Sause, R., and Fahnestock, L. A. (2001). "Strength and ductility of HPS-100W I-girders in negative flexure." *J. Bridge Eng.*, 6(5), 316–323.

White, D. W., Zureick, A. H., Phoawanich, N. P., and Jung, S. K. (2001). "Development of unified equations for design of curved and straight steel bridge I girders," *Final Rep. to American Iron and Steel Institute*, Professional Service Industries, Inc., and Federal Highway Administration, Washington, D.C.